Local Electronic Structure of Olivine Phases of Li_xFePO_4

Shu Miao,*,†,§ Michael Kocher,‡ Peter Rez,‡ Brent Fultz,†,§ Rachid Yazami,†,§ and Channing C. Ahn†,§

California Institute of Technology, Pasadena, California 91125, Arizona State University, Tempe, Arizona 85287-1504, and CNRS Caltech International Laboratory, Pasadena, California 91125

Received: December 14, 2006; In Final Form: February 25, 2007

Changes in the local electronic structure at atoms around Li sites in the olivine phase of $LiFePO_4$ were studied during delithiation. Electron energy loss spectrometry was used for measuring shifts and intensities of the near-edge structure at the *K*-edge of O and at the *L*-edges of P and Fe. Electronic structure calculations were performed on these materials with a plane-wave pseudopotential code and with an atomic multiplet code with crystal fields. It is found that both Fe and O atoms accommodate some of the charge around the Li^+ ion, evidently in a hybridized Fe−O state. The O 2p levels appear to be fully occupied at the composition $LiFePO_4$. With delithiation, however, these states are partially emptied, suggestive of a more covalent bonding to the oxygen atom in $FePO_4$ as compared to $LiFePO_4$. The same behavior is found for the white lines at the Fe $L_{2,3}$-edges, which also undergo a shift in energy upon delithiation. A charge transfer of up to 0.48 electrons is found at the Fe atoms, as determined from white line intensity variations after delithiation, while the remaining charge is compensated by O atoms. No changes are evident at the P $L_{2,3}$-edges.

Introduction

The olivine phase of $LiFePO_4$ is drawing much interest as a promising cathode material for rechargeable lithium ion batteries. It is nontoxic, nonhygroscopic, chemically stable, environmentally friendly, and inexpensive.[1−3] It has a discharge voltage of 3.5 V vs Li/Li^+ and a high theoretical capacity of 170 mAh/g. The small volumetric expansion and structural changes during Li^+ insertion and extraction are believed to be beneficial to a high cycle life.[4] There are problems with its low electronic conductivity, but there are practical approaches to improving conductivity by doping with supervalent cations[5] or carbon coating[6,7] or by reducing the particle size.[8]

$LiFePO_4$ occurs in nature as the mineral triphylite, and its delithiated counterpart, $FePO_4$, is known as heterosite. At room temperature, both phases are olivine type orthorhombic structures. Lithium atoms are present as chains in the channels along the *b*-axis in $LiFePO_4$.[1,2] For intermediate compositions of lithium in Li_xFePO_4, where $0 < x < 1$, the material is a two-phase system consisting of both heterosite and triphylite in proportions consistent with the overall lithium content.[1] Recently, Yamada et al. suggested that Li_xFePO_4 is a mixture of $Li_{0.05}FePO_4$ and $Li_{0.89}FePO_4$.[9] At temperatures around 350 °C, a new disordered phase appears, having the same olivine structure and lattice parameters intermediate between those of heterosite and triphylite.[10] Lithium atoms are distributed uniformly in this new solid solution phase at high temperatures.

Theoretical and experimental work has been done to understand the electronic structure and phase transitions in $LiFePO_4$ during lithium insertion and extraction. The charge compensation and phase separation in the electrochemical lithiation reaction are generally attributed to the reduction of Fe^{3+} to Fe^{2+}.[1,11,12] It has been suggested that the PO_4^{3-} polyanion lowers the Fermi level and hence raises the cell potential and maintains a stable structural framework through strong P−O covalent bonds.[2,3,13,14] Density functional theory (DFT) calculations show that Fe 3d states dominate the bottom of the conduction bands in both $LiFePO_4$ and $FePO_4$. The unoccupied Fe 3d states may have more mixing with O 2p states in $FePO_4$ than in $LiFePO_4$.[15] Unfortunately, the two-phase region of the phase diagram is not predicted by standard DFT methods, although DFT+U methods give more accurate predictions of the phase diagram and electrochemical potentials.[12,16]

The shift of the Fe *K*-edge of up to 4.3 eV during delithiation, observed using in situ X-ray absorption spectroscopy (XAS), has been attributed to oxidation of Fe^{2+} to Fe^{3+}.[17] Mössbauer spectroscopy also provides evidence for transitions between Fe^{2+} and Fe^{3+} during lithiation and delithiation.[18] A study of the valence-related Fe 3d electronic states was performed with soft X-ray absorption and emission spectroscopies.[15] An upward shift of about 2 eV at the Fe L_3 peak and a stronger bonding character of the Fe 3d and O 2p orbitals were detected after delithiation. These changes were attributed to the Fe^{2+} to Fe^{3+} oxidation and a large charge transfer from ligand O 2p to Fe 3d states. High-resolution electron energy loss spectroscopy (EELS) measurements also showed a shift of Fe *L*-edges and the presence of a new peak at the O *K*-edge after delithiation.[19] Peaks at the *L*-edges in the EELS spectra of transition metals are called white lines because they were originally observed as overexposed regions on the photographic film used to record XAS spectra.[20] These intense sharp peaks represent electronic transitions from occupied 2p core states to empty 3d states.

In this paper, we quantify the charge compensation during lithium extraction from $LiFePO_4$ by using EELS with computational support. A shift of 1.4 eV at Fe white lines is detected after delithiation. Quantification of the near-edge structure at Fe white lines and the O *K*-edge shows that the Fe and O atoms play equal roles in charge compensation upon delithiation.

* To whom correspondence should be addressed. E-mail: shu@caltech.edu.
† California Institute of Technology.
‡ Arizona State University.
§ CNRS Caltech International Laboratory.

10.1021/jp068605q CCC: $37.00
Published on Web 04/20/2007

Experimental

Powders of $LiFePO_4$ were prepared by a solid-state reaction. Iron oxalate [$Fe(C_2O_4)\cdot 2H_2O$], ammonium dihydrogen phosphate ($NH_4H_2PO_4$), and lithium carbonate (Li_2CO_3) were mixed in the molar ratio 1:1:0.5 and then ball milled in acetone for 12 h. The paste was dried at 60 °C in vacuum. The mixture was then reground and heated in a nitrogen atmosphere at 700 °C for 24 h. Aqueous potassium persulfate ($K_2S_2O_8$) solution was used to chemically delithiate $LiFePO_4$ to achieve $Li_{0.6}FePO_4$ and $FePO_4$. Measurements on individual crystals of $Li_{0.6}FePO_4$ may not properly reflect the overall composition because the crystal may contain only one phase of the two-phase mixture. To achieve chemical homogeneity in the partially delithiated material, the $Li_{0.6}FePO_4$ powder was prepared as a disordered solid solution by heating to 380 °C in an evacuated glass ampule and quenching the sealed ampule into water, as described elsewhere.[21]

X-ray diffraction (XRD) patterns were measured with a Philips PW3040-Pro diffractometer using Cu Kα radiation ($\lambda = 0.15046$ nm). Silicon powder was mixed with the samples as a standard to ensure accuracy in peak position determination. Rietveld refinement was then used to determine the compositions and structures.

For transmission electron microscopy analysis, the samples were crushed with a mortar and pestle in alcohol and the powder was dispersed on a holey carbon grid. EELS data were acquired using a postcolumn Gatan 666 parallel EELS spectrometer installed on a Philips EM420 electron microscope operating at 100 kV. The typical area of analysis is about 10^4 nm^2, which was sufficiently large to average out the possible compositional fluctuations within the examined particles. The energy resolution was about 1.5 eV with an energy dispersion of 0.5 eV per channel. The experimental spectra were deconvoluted using a Fourier-log method to remove plural scattering.[22] A power-law fit was performed to the background just before the onset of each ionization edge, and the estimated background was then subtracted from the data.[23]

Electronic Structure Calculations

Calculations of the electronic structure were performed for a four-formula unit cell for Li_xFePO_4 ($x = 1$ and 0). The VASP[24,25] (Vienna ab initio simulation program) code was used with projector augmented wave potentials in the generalized gradient approximation. Calculations were performed for both ferromagnetic and antiferromagnetic configurations of the iron atoms. Following Zhou et al.,[16,26] we also examined the effect of the self-energy U, which was set to 4.3 eV. The initial coordinates were taken from Tang and Holzwarth,[27] and a full relaxation of the unit cell and atomic positions was performed. A plane wave energy cutoff of 500 eV was used in conjunction with a $9 \times 2 \times 7$ k point grid (corresponding to 20 irreducible k points) to obtain an energy convergence to 0.001 eV/atom. For density of states (DOS) calculations, the atom positions were taken from a converged calculation and the number of bands calculated was increased to 130. The DOS was evaluated by convoluting appropriately weighted individual band energies at each k point with a Gaussian of width 1.5 eV, giving a resolution that matched the experimental data.

To understand possible charge transfers, it is useful to apportion the total charge among the different atoms in the unit cell. This can be done in various ways. One accepted technique is to calculate the charge in spheres centered at the atom positions. Because there is no rigorous procedure for selecting sphere size, the relative charge associated with each atom, or for that matter the division of charge between atoms and an interstitial region, can be arbitrary. Instead, we have chosen to follow the procedure of Bader,[28] where the division is made along contour lines following the interatomic peaks in the charge density. This gives an unambiguous division of charge among the unit cell constituent atoms.

Features in the EELS fine structures of transition metal compounds can be influenced by both atomic and solid-state electronic effects. The shapes of transition metal $L_{2,3}$-edges can be altered significantly by atomic multiplets arising from the overlap of the radial wave functions for the 2p hole and holes in the partially filled 3d band. Final states must be calculated by vector coupling of the 2p and 3d wave functions. This strong, purely atomic, effect is only partly screened in the solid state, meaning that features in spectra are comparable for solids and isolated atoms. The initial and final states are specified as a sum of terms in the LS coupling scheme. For example, for Fe^{2+}, the initial state configuration would be $2p^63d^6$ and the final state would be $2p^53d$.[7] The initial ground state $^5D_2$ is given by Hund's rule. Transitions calculated with a dipole selection rule give ΔJ as -1, 0, 1. In this case, there are 110 terms allowed for the final state, giving 68 distinct transitions. The strengths of the various transitions are calculated from the appropriate matrix elements from the Hamiltonian.

$$H = \sum_N \frac{p_i^2}{2m} + \sum_N \frac{-Ze^2}{r_i} + \sum_{\text{pairs}} \frac{e^2}{r_{ij}} + \sum_N \zeta(r_i) l_i s_i$$

The first two terms of this Hamiltonian, the kinetic energy and the electron−nuclear Coulombic interaction, are the same for all electrons in a configuration. Only the last two terms, the electron−electron interaction and the spin−orbit coupling, need to be considered. In practice, for transition element ions, it has been found necessary to reduce the pd exchange integrals by 20% from the values calculated using the Hartree−Fock wave functions.

The oxygen atoms neighboring the Fe ion add a crystal field that is represented as a sum of spherical harmonics and can be treated as a perturbation to the atomic multiplet calculation. The main effect is to change the local symmetry from spherical to octahedral. The strength of this crystal field is specified by 10Dq, which can be determined from the separation between the t_{2g} and the e_g molecular orbitals. Because contributions from these orbitals could not be directly identified from the densities of states, we varied 10Dq between 1 and 3.5 eV to best match the experimental Fe $L_{2,3}$-spectrum. Calculations of some transition metal white line intensities in octahedral and tetrahedral symmetry are given by Van der Laan and Kirkman.[29] A detailed description of multiplet theory applied to inner shell spectroscopy can be found in the review by de Groot,[30] whose codes were used in the present work.

Results

At room temperature, XRD patterns of $LiFePO_4$ and $FePO_4$ are readily indexed as single-phase triphylite and heterosite (Figure 1). The diffraction pattern from the disordered $Li_{0.6}FePO_4$ is also characteristic of a single-phase material. Figure 1 indicates that the quenched material preserves its disordered structure well at room temperature, because of the sluggish kinetics of the unmixing process at temperatures below 200 °C.

Figure 2 shows EELS measurements of P $L_{2,3}$-edges of the samples. The peak positions and fine structures are similar for

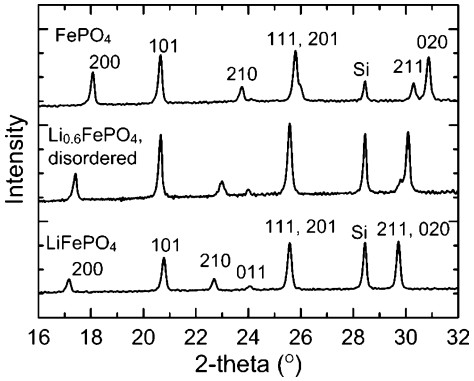

Figure 1. Indexed X-ray powder diffraction patterns from samples of Li_xFePO_4 with different states of lithiation, with Si as an internal standard.

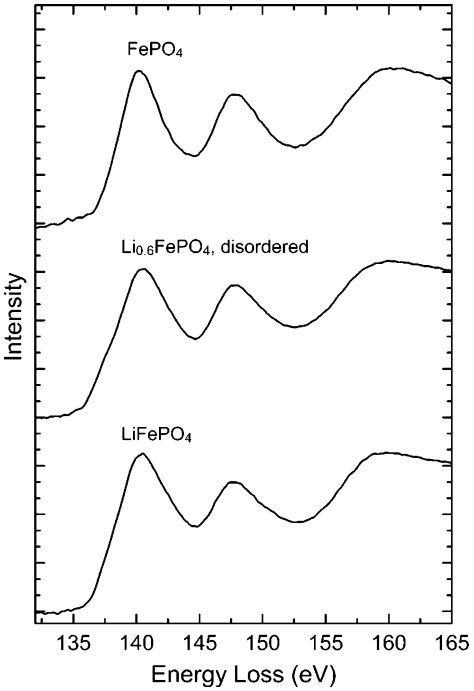

Figure 2. P $L_{2,3}$-edge from Li_xFePO_4. The spectra were normalized with a 50 eV window after the L_2 peak.

all samples. No changes in these P spectra were observed during delithiation or thermal treatment. The low-energy EELS spectra in Figure 3 are complicated by the overlap of the Li *K*-edge and Fe $M_{2,3}$-edge. Quantification is not possible, but qualitative features are visible. The peaks in this area (indicated as A, B, and C) vary in their intensities and shapes. Peak A at 55 eV and peak C at 65 eV in the triphylite phase belong to the Li *K*-edge, so the intensities of these features give semiquantitative information about the Li content in the material. These features are less evident in the disordered sample than in $LiFePO_4$. Peak B around 58 eV contains significant contributions from both the Li *K*-edge and the Fe $M_{2,3}$-edge. It is broad in the fully lithiated $LiFePO_4$ and becomes sharper in the disordered phase containing less lithium. This peak actually grows during delithiation, indicating that Fe $M_{2,3}$-edge may gain intensity when lithium is extracted from the materials.

Figure 4 shows a change in the O *K*-edge with delithiation. A prepeak (labeled A) at 528 eV is found in the delithiated material. It is almost negligible in the triphylite ($LiFePO_4$) but is distinct in the fully delithiated sample. In the disordered sample with composition $Li_{0.6}FePO_4$, this prepeak is also present but its intensity is only 27% of that in the heterosite phase. The

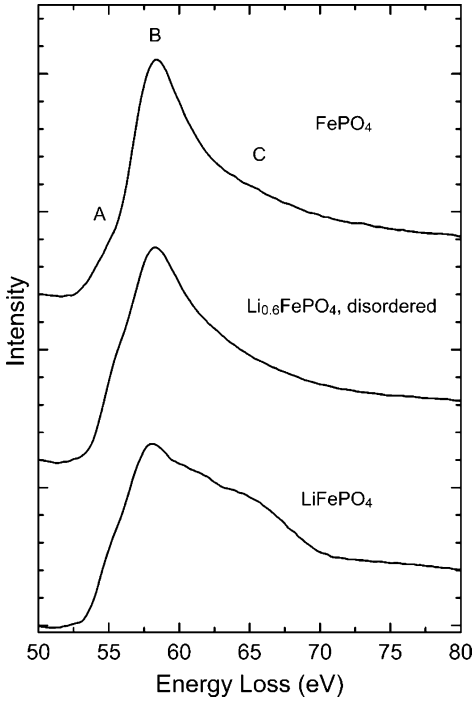

Figure 3. Li *K*-edge and Fe $M_{2,3}$-edge from Li_xFePO_4. The spectra were normalized with a 50 eV window after the peak.

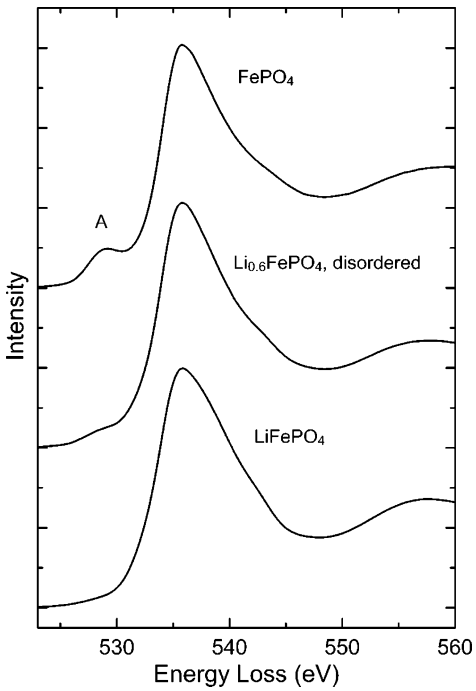

Figure 4. O *K*-edge from Li_xFePO_4. The spectra were normalized with a 40 eV window after the main peak.

main peak of the O *K*-edge (531−547 eV with a maximum at 535.6 eV) is similar for all samples.

Figure 5a shows changes in the Fe white lines with delithiation. The intensities of the sharp lines themselves scale with the number of unoccupied 3d states at the Fe atom.[31,32] The intensity under the white lines contains contributions from excitations to both 3d bound states and continuum states. The continuum contribution was determined by using a two-segment line model to extract the bound state contribution accurately.[32] With delithiation, the Fe white lines also undergo an upward shift in energy. The centroid of the L_3 peak is plotted in Figure 5b. In the fully delithiated heterosite phase, the shift is 1.4 eV.

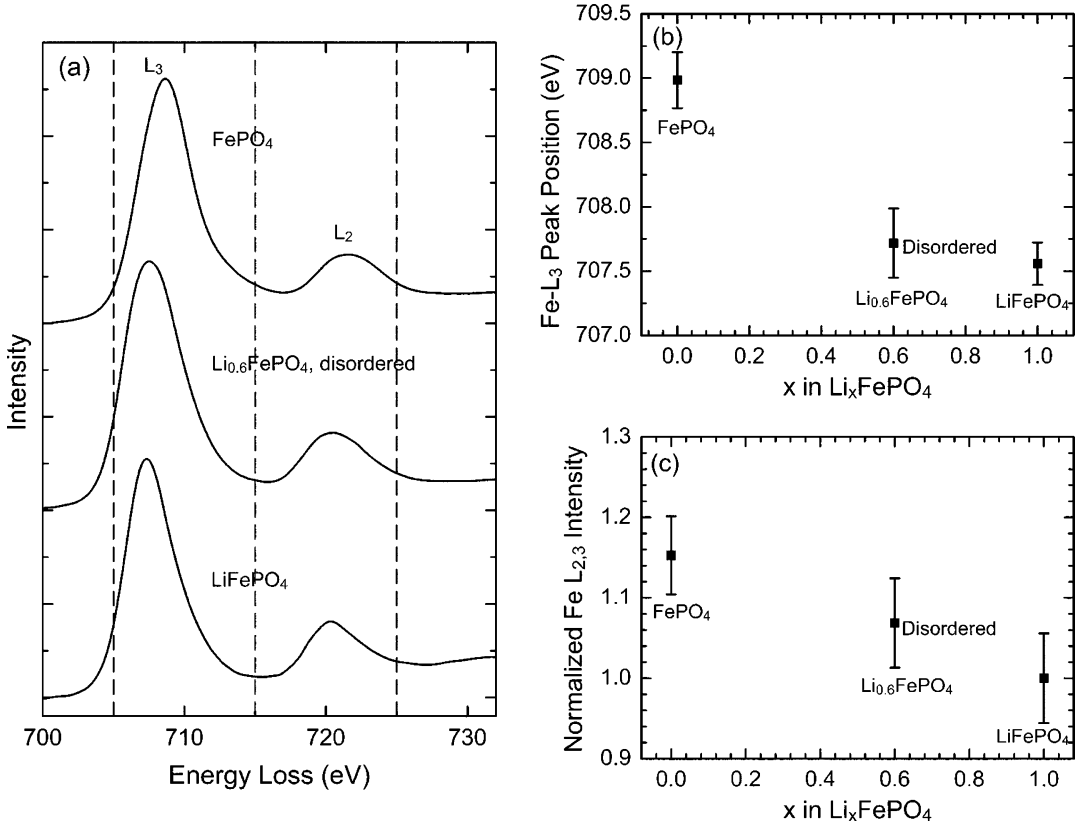

Figure 5. (a) Fe $L_{2,3}$-edges from Li_xFePO_4. The spectra were normalized with a 40 eV window after the L_2 peak. The measured shift of the L_3 centroid and the normalized white line intensities are plotted in parts b and c.

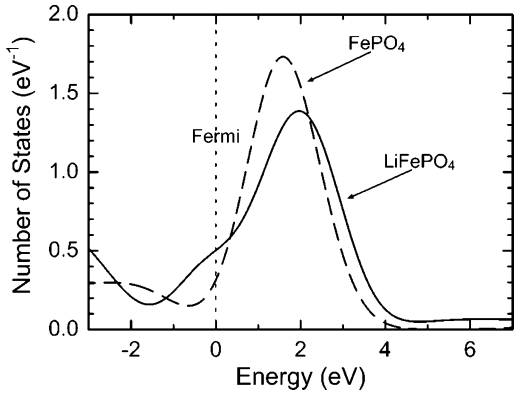

Figure 6. VASP calculation of Fe 3d partial DOS per formula unit. The intensity above the Fermi level corresponds to the intensity of white lines in EELS spectra. A 14% increase of the unoccupied states from $LiFePO_4$ to $FePO_4$ is predicted.

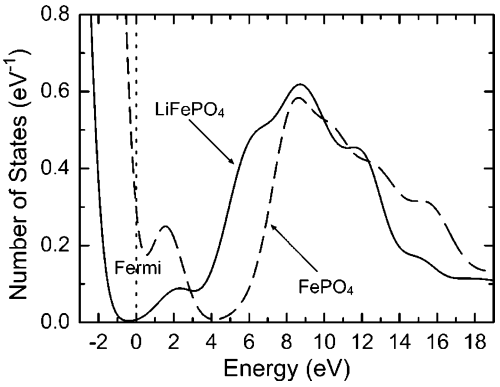

Figure 7. VASP calculation of the O 2p partial DOS per formula unit. The intensity from 0 to 3 eV above the Fermi level corresponds to the intensity of the experimental prepeak.

A variation of Fe white line intensity is also observed (Figure 5c). From $x = 1$ to $x = 0$, the total intensity of the L_2 and L_3 white lines increases by 15%, indicating a depletion of Fe 3d electrons, while the increase is about 7% in the disordered sample of $Li_{0.6}FePO_4$.

The calculated densities of Fe d states and O p states of one formula unit for $LiFePO_4$ and $FePO_4$ in the antiferromagnetic configuration for $U = 4.3$ eV are shown in Figures 6 and 7, respectively. At the resolution of the experimental data, which was matched in the calculations, no differences could be seen between densities of states for ferromagnetic and antiferromagnetic configurations or for different values of U. Charges associated with the oxygen and iron atoms as given by the Bader analysis are presented in Table 1. There is a loss of one electron from $LiFePO_4$ to $FePO_4$ per chemical formula, indicating that only Fe and O contribute to the charge compensation. Multiplet calculations for Fe^{2+} and Fe^{3+} are shown in Figure 8. Setting 10Dq to 3 eV gives the best fit to the experimental peak shape. The shift between the centroids of Fe^{2+} and Fe^{3+} L_3 peaks is then 1.87 eV.

Discussion

Significant changes were observed at the Fe white lines after delithiation. The upward shift of about 1.4 eV after delithiation indicates an increase in the difference between the bonding energy of the localized Fe 2p levels and the outer delocalized Fe 3d levels in the materials. Such a shift can be caused by a valence change of the atom, although changes in the structural and chemical environment surrounding the atom can cause small shifts in white lines. The shift between the L_3 peaks for Fe^{2+} and Fe^{3+} is 1.87 eV when calculated using the atomic multiplets codes with 10Dq set at 3 eV. This is in reasonable agreement

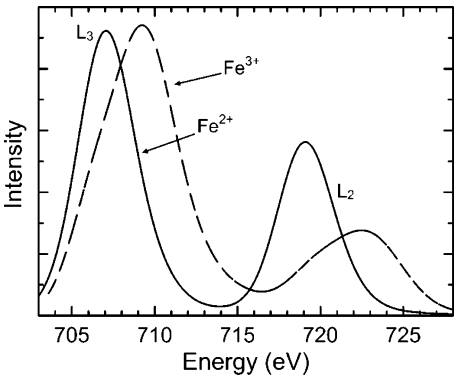

Figure 8. Atomic multiplet calculation of Fe $L_{2,3}$ white lines.

TABLE 1: Bader Analysis of the Number of Electrons Surrounding O and Fe Atoms Per Li_xFePO_4 ($x = 0, 1$)

	O	Fe
$LiFePO_4$	31.55	6.46
$FePO_4$	31	6.01
difference	0.55	0.45

with the experimental value of 1.4 eV (Figure 8). The atomic multiplet approach is best-suited to describing systems that are mainly ionic in character, with limited covalent bonding to nearest neighbors described by the crystal field. This might not apply to the $LiFePO_4$, $FePO_4$ system, as partly evidenced by the large value of 10Dq needed to bring about some measure of agreement with experiment. We therefore expect less than a full electron transfer to the Fe atom with lithiation. This may also be the cause of the discrepancy between the intensity of the L_2 peak of the experimental and calculated spectra.

More information about the electronic states of Fe atoms is available from the intensities of the normalized Fe white lines. The total white line intensity of the $FePO_4$ phase is 15% larger than that of the $LiFePO_4$ phase. This indicates that with delithiation, more electrons are removed from the Fe 3d levels, and Fe^{2+} is oxidized to a higher valence. This is in agreement with the VASP electronic structure calculations that show a 14% increase in the proportion of unoccupied d states when going from $LiFePO_4$ to $FePO_4$ (Figure 6). There are 3.2 holes in the Fe 3d states per formula unit in $LiFePO_4$ as indicated by the VASP calculations. A 15% increase of white line intensity corresponds to a depletion of 0.48 electrons per Li atom. From the pseudopotential computational work, the Bader analysis of the charge density from the VASP calculations shows that the iron is responsible for 45% of the charge compensation. Evidently, Fe atoms are not responsible for all of the charge compensation in $LiFePO_4$ during delithiation and lithiation.

In the disordered sample of $Li_{0.6}FePO_4$, the increase of the white line intensity is about 7%, corresponding to a removal of 0.22 electrons. Considering that 0.48 electrons are removed in fully delithiated $FePO_4$, this value is consistent with the overall composition.

At the O *K*-edge, the most visible change with delithiation is the increase in the prepeak intensity at 528 eV. This prepeak originates from electron transitions from a 1s core state to states with 2p character at oxygen atoms. Because the number of available holes in these 2p states is determined by the extent of the orbital hybridization with adjacent atoms, this prepeak provides information on the bonding of the oxygen atoms.[33] In $LiFePO_4$, the prepeak is not present, indicating that all six 2p states of oxygen atoms are fully occupied. No 1s to 2p transition can occur. In the fully delithiated $FePO_4$ phase, the prepeak intensity increases significantly, indicating more hybridization between oxygen and surrounding atoms, and more covalent bonding. The prepeak is also visible in the VASP calculations of the oxygen p DOS (Figure 7). The calculated ratio of prepeak to integrated p DOS, from 3 to 14 eV above the Fermi level, is 14%, which can be compared directly to the experimental measurement of 8% in the same energy range, since the matrix element for the inelastic scattering slowly varies over this small range of energy. These results also agree with results from soft XAS measurements.[15] The prepeak in the disordered sample of $Li_{0.6}FePO_4$ is about 27% of that in the $FePO_4$ phase, showing a reasonable trend with lithiation as the extra electrons associated with the Li^+ are accommodated in part by O 2p states that are more covalently bonded to Fe. The oxygen atoms in $LiFePO_4$ and $FePO_4$ have three inequivalent sites.[18] EELS measurements cannot separate these three contributions. Nevertheless, because no changes are observed at the P *K*-edge and the P−O bonds have been shown to undergo minimal shrinking during lithium removal,[18] we expect that the increase of the prepeak intensity is contributed mainly by the oxygen atoms bonded to Fe. We therefore suggest that the electron removed with Li^+ during delithiation is donated by electronic states that are hybrids of the O 2p and Fe 3d states.

Conclusions

The olivine phases of triphylite $LiFePO_4$, heterosite $FePO_4$, and a disordered solid solution of $Li_{0.6}FePO_4$ were studied by EELS and electronic structure calculations. A shift of about 1.4 eV at Fe white lines was detected after delithiation. A charge transfer up to 0.48 electrons from iron is observed from the variation in the experimental Fe white line intensity. Both experimental and theoretical data show oxidation of Fe after delithiation. Electronic structure calculations and the presence of a prepeak on the oxygen *K*-edge of $FePO_4$ indicate that only about half of the charge compensation takes place on the iron atoms while the remainder takes place on oxygen atoms. The 2p states at oxygen atoms are fully occupied in $LiFePO_4$, but there is some emptying of these states in the delithiated material. The oxygen atoms are more covalently bonded in $FePO_4$ than in $LiFePO_4$. Finally, we observed that the high-temperature disordered phase of $Li_{0.6}FePO_4$ was kinetically stable at room temperature.

Acknowledgment. This work was supported by the U.S. Department of Energy under Grants DEFG0300ER15035 and DEFG0203ER15425.

References and Notes

(1) Padhi, A. K.; Nanjundaswamy, K. S.; Goodenough, J. B. *J. Electrochem. Soc.* **1997**, *144*, 1188.

(2) Padhi, A. K.; Nanjundaswamy, K. S.; Masquelier, C.; Okada, S.; Goodenough, J. B. *J. Electrochem. Soc.* **1997**, *144*, 1609.

(3) Yamada, A.; Chung, S. C.; Hinokuma, K. *J. Electrochem. Soc.* **2001**, *148*, A224.

(4) Deb, A.; Bergmann, U.; Cramer, S. P.; Cairns, E. J. *Electrochim. Acta* **2005**, *50*, 5200.

(5) Chung, S. Y.; Bloking, J. T.; Chiang, Y. M. *Nat. Mater.* **2002**, *1*, 123.

(6) Huang, H.; Yin, S. C.; Nazar, L. F. *Electrochem. Solid-State Lett.* **2001**, *4*, A170.

(7) Chen, Z.; Dahn, J. R. *J. Electrochem. Soc.* **2002**, *149*, A1184.

(8) Yamada, A.; Chung, S. C.; Hinokuma, K. *J. Electrochem. Soc.* **2001**, *148*, A224.

(9) Yamada, A.; Koizumi, H.; Nishimura, S. I.; Sonoyama, N.; Kanno, R.; Yonemura, M.; Nakamura, T.; Kobayashi, Y. *Nat. Mater.* **2006**, *5*, 357.

(10) Delacourt, C.; Poizot, P.; Tarascon, J. M.; Masquelier, C. *Nat. Mater.* **2005**, *4*, 254.

(11) Burba, C. M.; Frech, R. *J. Electrochem. Soc.* **2004**, *151*, A1032.

(12) Zhou, F.; Marianetti, C. A.; Cococcioni, M.; Morgan, D.; Ceder, G. *Phys. Rev. B* **2004**, *69*, 201101.
(13) Padhi, A. K.; Nanjundaswamy, K. S.; Masquelier, C.; Goodenough, J. B. *J. Electrochem. Soc.* **1997**, *144*, 2581.
(14) Masquelier, C.; Padhi, A. K.; Nanjundaswamy, K. S.; Goodenough, J. B. *J. Solid State Chem.* **1998**, *135*, 228.
(15) Augustsson, A.; Zhuang, G. V.; Butorin, S. M.; Osorio-Guillén, J. M.; Dong, C. L.; Ahuja, R.; Chang, C. L.; Ross, P. N.; Nordgren, J.; Guo, J. H. *J. Chem. Phys.* **2005**, *123*, 184717.
(16) Zhou, F.; Kang, K.; Maxisch, T.; Ceder, G.; Morgan, D. *Solid State Commun.* **2004**, *132*, 181.
(17) Haas, O.; Deb, A.; Cairns, E. J.; Wokaun, A. *J. Electrochem. Soc.* **2005**, *152*, A191.
(18) Andersson, A. S.; Kalska, B.; Häggström, L.; Thomas, J. O. *Solid State Ionics* **2000**, *130*, 41.
(19) Laffont, L.; Delacourt, C.; Gibot, P.; Wu, M. Y.; Kooyman, P.; Masquelier, C.; Tarascon, J. M. *Chem. Mater.* **2006**, *18*, 5520.
(20) Veldkamp, J. *Physica* **1935**, *2*, 25.
(21) Dodd, J. L.; Yazami, R.; Fultz, B. *Electrochem. Solid-State Lett.* **2006**, *9*, A151.
(22) Johnson, D. W.; Spence, J. C. H. *J. Phys. D* **1974**, *7*, 771.
(23) Egerton, R. F. *Electron Energy-Loss Spectroscopy in the Electron Microscope*; Plenum: New York, 1996.
(24) Kresse, G.; Furthmuller, J. *Phys. Rev. B* **1996**, *54*, 11169.
(25) Kresse, G.; Joubert, D. *Phys. Rev. B* **1999**, *59*, 1758.
(26) Zhou, F.; Cococcioni, M.; Marianetti, C. A.; Morgan, D.; Ceder, G. *Phys. Rev. B* **2004**, *70*, 235121.
(27) Tang, P.; Holzwarth, N. A. W. *Phys. Rev. B* **2003**, *68*, 165107.
(28) Bader, R. F. W. *Atoms in Molecules: A Quantum Theory*; Oxford University Press: New York, 1994.
(29) Van der Laan, G.; Kirkman, I. W. *J. Phys.: Condens. Matter* **1992**, *4*, 4189.
(30) de Groot, F. *Coord. Chem. Rev.* **2005**, *249*, 31.
(31) Starace, A. F. *Phys. Rev. B* **1972**, *5*, 1773.
(32) Pearson, D. H.; Fultz, B.; Ahn, C. C. *Appl. Phys. Lett.* **1988**, *53*, 1405.
(33) de Groot, F.; Grioni, M.; Fuggle, J. C.; Ghijsen, J.; Sawatzky, G. A.; Petersen, H. *Phys. Rev. B* **1989**, *40*, 5715.